

Experimental Analyses of the Evaporation Dynamics in Bare Soils under Natural Conditions

Alessia Flammini¹  · Corrado Corradini¹ · Renato Morbidelli¹ · Carla Saltalippi¹ · Tommaso Picciafuoco¹ · Juan Vicente Giráldez^{2,3}

Received: 9 December 2016 / Accepted: 14 November 2017 /

Published online: 21 November 2017

© Springer Science+Business Media B.V., part of Springer Nature 2017

Abstract In spite of recent progresses in evaporation estimate through advanced models and laboratory experiments, the drying process of bare soils through its successive stages remains difficult to predict. A study which addresses evaporation modeling in natural bare soils is presented. It relies upon hydro-meteorological measurements performed in a plot with a bare silt loam soil maintained in natural conditions. The following steps are involved: estimate of daily actual evaporation, E_a , through the hydrological balance, scaling with pan evaporation measurements, E_{pan} , and analysis of the relation of E_a/E_{pan} with the soil moisture vertical profile. The results enable us (1) to check the occurrence of the first stage of the evaporation process, characterized by not limited-soil water supply and high evaporative rates, and (2) to identify the transition from the first to the second stage, with decreasing soil water-limited E_a values. The last point requires the introduction of a soil water content threshold at 5 cm depth, that is associated with the soil field capacity. The adopted procedure provides insights on the soil water dynamics at depths differently involved through the successive stages of the evaporative process. Finally, indications on the use of pan evaporation measurements in evaporative rate estimate at least during the first stage of the process are also given.

Keywords Evaporation dynamics · Hydrological balance · Soil water content · Bare soil

✉ Alessia Flammini
alessia.flammini@unipg.it

¹ Department of Civil and Environmental Engineering, University of Perugia, via G. Duranti 93, 06125 Perugia, Italy

² Department of Agronomy, University of Cordoba, da Vinci Bldg, km 396 Cra, Madrid, Spain

³ Department of Agronomy, Institute for Sustainable Agriculture, CSIC, Alameda del Obispo, Córdoba, Spain

1 Introduction

Evaporation is one of the most important processes of the global hydrological cycle. It involves mass and heat exchanges between land and atmosphere and directly affects the groundwater resources and water management (Banimahd et al. 2016; Balugani et al. 2016). About 60% of terrestrial precipitation supplies the evaporative process that takes place through direct evaporation from soil surface (20%) and plant transpiration (40%) (Or et al. 2013). Evaporation from the surface of porous media is driven by the atmospheric evaporative demand, linked with the radiative transfer and aerodynamic transport depending on the combined effects of wind speed, air temperature and atmospheric humidity (McVicar et al. 2012). Furthermore, the evaporative process can be limited by a soil water content insufficient to satisfy the phase change from liquid to vapor required by the actual evaporative demand (Or et al. 2013).

In any case, evaporation is a phenomenon that remains difficult to predict because of the complex interactions between soil and atmosphere.

In the last 10 years several advanced models based on the standard continuum approach have been proposed to describe liquid water, vapor and heat movement in bare soils. Typically, this approach, for the first time represented by a model developed by Philip and de Vries (1957), involves numerical solutions that describe the non-isothermal combined transport of liquid water, water vapor, gas and heat in terms of mass conservation, under the hypothesis of liquid-vapor equilibrium (Grifoll et al. 2005; Bittelli et al. 2008; Novak 2010). In the afore mentioned models, mainly tested through laboratory trials or highly controlled field experiments (Bittelli et al. 2008; Grifoll et al. 2005; Novak 2010), the evaporation rate is one of the surface boundary conditions, that is usually expressed as a function of the boundary layer soil resistance and of soil water vapor density deficit between the soil surface and a “screen height”. Furthermore, the estimate of a few parameters for liquid water, water vapor and energy balance is required. These elements make difficult the application of such formulations in most natural conditions, even though important indications on the gradual drying process of bare soils have been obtained.

In the scientific literature much attention has been also addressed to the study of the different stages of evaporation process in bare soils, characterized by vertical profiles both homogeneous (Bittelli et al. 2008; Lehmann et al. 2008; Shokri et al. 2012; Or et al. 2013) and layered (Shokri et al. 2010; Assouline et al. 2014). These studies, usually based on laboratory experiments, suggest that the evaporation process from an initially saturated bare soil under non-limiting energy conditions involves successive stages. Specifically, for example Lemon (1956) pointed out the existence of: a first stage with evaporation rate equal to the potential value until a critical point; a second stage with decreasing evaporation rate while soil dries and loses the capability to drive water up to the surface and a third stage characterized by very low evaporation rates influenced by soil physical characteristics.

The first stage, also defined the “constant rate period” because the evaporation rate is expected to remain constant if the external demand is time-invariant, is characterized by non-limiting soil water supply with soil hydraulic continuity supported by capillarity, which is maintained also for decreasing surface soil water content. In the successive stages, also called “falling rate period”, firstly the transport of both liquid and vaporized water occurs while the hydraulic continuity is still partially maintained, then the moisture transport is only due to the gaseous phase (Lehmann et al. 2008).

The passage through different stages is linked with the dynamics of the drying front, identified as the interface between completely and partially liquid-filled pores, and considered as the top of capillarity fringe in Lehmann et al. (2008). As far as a film region between the drying front and the soil surface is maintained, evaporation rate assumes the potential value; when the liquid connections decrease also the capability of soil to supply water to the surface decreases causing a falling evaporation rate, until the liquid connections are disrupted. Then, the evaporative surface drops below the soil surface with formation of an air-filled layer, where moisture transport occurs only through water vapor, producing very low evaporation rates. The dynamics of the drying front can be related to the evaporation characteristic length defined as the maximum height of liquid continuity through the unsaturated zone. The characteristic length is a soil property linked with the width of pore size distribution and can be derived from the retention curve (Lehmann et al. 2008; Or et al. 2013).

A few studies indicate that in most arid regions evaporation from bare soils mainly involves the first two stages that could be accurately represented (Idso et al. 1974).

The main objective of this paper is to propose an experimental methodology useful to improve the evaporation modeling in natural bare soils. Specifically, examining the soil depth involved in each stage of the evaporation process, a procedure to identify the first two stages of the evaporation process on the basis of the soil water content observed at a significant depth is proposed. In this context the soil field capacity, estimated by a functional form of the soil retention curve, is considered as an indicator of the onset of the second evaporation stage. In our analysis the actual evaporation was obtained by the hydrological balance equation applied in a plot with a bare silt loam soil where measurements of rainfall, soil water content, surface-, intermediate- and deep- flows were available; pan evaporation was used as a surrogate of potential evaporation.

2 Monitoring System

The investigation here presented relies upon measurements performed in a plot close to the University of Perugia (Central Italy) during the hot seasons of years 2010, 2013 and 2014. The experimental system consists of:

- a hydro-meteorological station including a Class A evaporation pan, subjected to a proper maintenance (Allen et al. 1998), and a rain gauge operative 2 m above the soil surface, with time resolution of 5 min;
- 9 × 9 m natural plot with slight slope, equipped with sensors for continuous measurements of the soil moisture vertical profile and surface-, intermediate- and deep- flows (Fig. 1).

The plot was artificially made by a granulometric selection of different natural soils properly meshed in order to obtain a vertically homogeneous soil, with a depth of 70 cm, and an underlying drainage layer with thickness of 10 cm. It was also laterally bounded in order to avoid lateral fluxes. The study soil, which belongs to the silt loam textural class (Linsley et al. 1992), is kept with a bare surface. The main

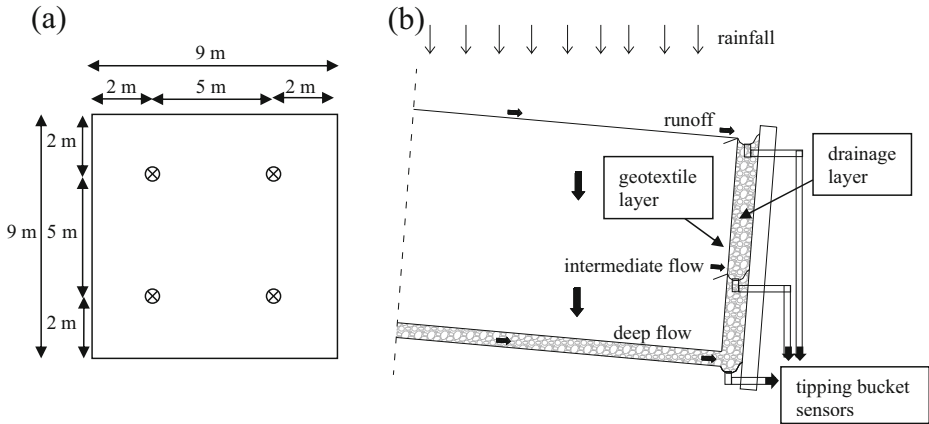


Fig. 1 Experimental plot: (a) layout with the four locations of the soil moisture measurements; (b) vertical section with the collectors of surface-, intermediate- and deep- flows

hydraulic properties are shown in Table 1. The values of the involved quantities are substantially similar to those earlier indicated by Morbidelli et al. (2011), with small adjustments made on saturated and residual soil water contents that have been updated to the maximum and minimum values, respectively, observed in the measurement points during the period from 2010 to 2014.

Four vertical profiles of soil moisture are monitored using the time-domain reflectometry (TDR) method (TRASE-BE, Soil Moisture Equipment Corp., Goleta, CA), with four three-rod waveguides of length 20 cm for horizontal insertion at 5, 15, 25 and 35 cm below the soil surface (Fig. 1a). The system as a whole can be used to monitor the water flow during infiltration, redistribution and re-infiltration. Data from the probes are recorded at 30 min intervals. The sensors were calibrated to convert the TDR signal into soil moisture.

Surface-, intermediate- (at about 40 cm depth) and deep- (at 70 cm depth) flows are continuously measured by 3 tipping bucket systems (Fig. 1b).

The adopted experimental conditions are expected to be well representative of the soil evaporation process under natural conditions because the tipping bucket sensor for the intermediate flow (see Fig. 1b) never detected the presence of appreciable discharges and this indicates that water flow along the direction parallel to the soil surface was of minor interest. On this basis, the distortion of the water flow could have affected only a narrow part of the plot very close to the downstream wall.

Table 1 Main characteristics of the study soil: θ_r and θ_s are the residual and saturated soil water contents, respectively, K_s is the saturated hydraulic conductivity, Ψ_b is the air entry head, λ is the Brooks–Corey pore size distribution index, c and d are empirical coefficients

| Soil components | Clay | Silt | Sand | USDA soil textural class | | | |
|----------------------|------------|------------|--------------|--------------------------|-----------|---|--------|
| (%) | 28 | 57 | 15 | silt loam | | | |
| Hydraulic properties | θ_r | θ_s | K_s (mm/h) | Ψ_b (mm) | λ | c | d (mm) |
| | 0.07 | 0.36 | 2 | -500 | 0.2 | 5 | 0 |

3 Methods

3.1 Hydrological Balance

The first step was the estimation of the daily actual evaporation, E_a , during the observation periods May–September 2010, June–July 2013, and May–October 2014. To this aim, the daily hydrological balance equation for the upper 70 cm of the soil depth was established as:

$$E_a = R - Q_s - Q_i - Q_d - S \tag{1}$$

where R is the measured rainfall depth, Q_s , Q_i , and Q_d were, respectively, the observed surface-, intermediate-, and deep- flows, and S the variation of the soil water depth computed from the measured water content profile. In particular, the last quantity was estimated through the following steps:

- first a time-varying horizontally averaged soil moisture content, $\bar{\theta}$, was determined at each soil depth $z = 5, 15, 25$ and 35 cm;
- then, the average soil moisture at different depths was interpolated through a step function to reproduce the entire wetting front at the beginning and the end of each day (Fig. 2);
- finally, the overall amount of soil water daily stored or released was derived using the wetting fronts available as a function of time (Fig. 2).

Figure 2 highlights that the soil water content observed at 35 cm depth was assumed to be representative of the lower soil layer. The decrease of soil water content with time in this layer was produced by soil water redistribution as a result of the existence of a small deep flow. Furthermore, the choice of a vertical profile constant with depth in the lower layer was

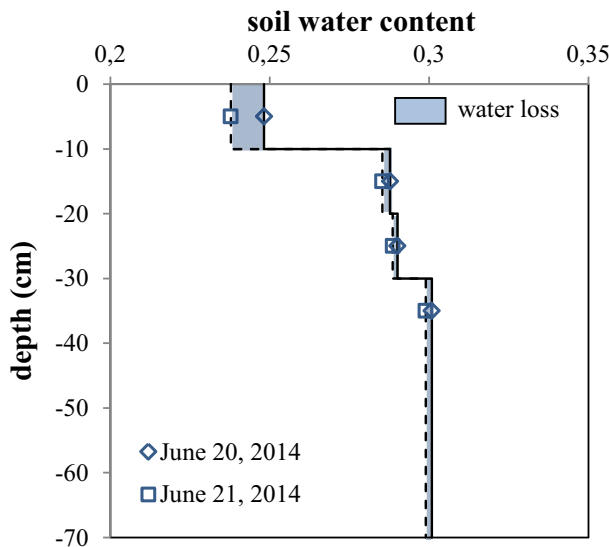


Fig. 2 Soil moisture observed at different depths in two successive days within a sample dry period (June 20–24, 2014) and vertical profile interpolated through a step function. The water loss due to evaporation and deep drainage is also shown

supported through the results obtained by an infiltration-redistribution model (Melone et al. 2006) earlier applied to the same plot (Morbidelli et al. 2011).

3.2 Scaled Actual Evaporation through Dry Periods

Since the purpose of this work is the analysis of soil evaporation processes, the considered time period was restricted to inter-storm events, when the cumulative actual evaporation approximately equals the water lost by soil. Rainfall records were used to characterize the dry period length (minimum duration 24 h) through a statistical analysis (Berretta et al. 2014) performed in the summer seasons of years 2009–2014. A Lognormal probability distribution function was fitted to the dry period lengths (χ^2 test - level of significance $\alpha = 0.10$), providing for 85% of cases expected dry period lengths up to 11 days. This value approximately matches the expected length of the first two evaporation stages in most arid regions (Bittelli et al. 2008).

Dry periods characterized by a length close to the aforementioned value were investigated, but our analysis is also representative for shorter dry periods which involve only partially the first two stages. The daily actual evaporation was expressed in a form independent of the atmospheric evaporative demand, that changes in function of external climatic conditions. Specifically, on a daily basis, E_a was normalized by simultaneous pan measurements, E_{pan} , available with time resolution of 30 min, adopted here as a surrogate of the potential evaporation rate, E_p . The use of the pan evaporation in this work was suggested by the need to establish an external reference not directly related to the soil itself since the first stage of evaporation is controlled by the atmospheric conditions. In addition, pan evaporation was considered to provide a good estimate of the external evaporative demand (Aminzadeh et al. 2016), was commonly adopted for agricultural and hydrological purposes (Rotsatyn et al. 2006) and was found to be linearly dependent on potential evaporation (Kahler and Brutsaert 2006).

The time evolution of the evaporative rate was investigated also through the method suggested by Brutsaert and Chen (1995) based on the assumption that the soil moisture-limited stage of evaporation can be treated as a desorption process with negligible gravity effects.

4 Analysis of Results

4.1 Investigation of the First two Stages of Evaporation Process

Because the characteristic length of a silt loam soil is expected to be in the range of 35–40 cm (Jalota and Prihar 1986; Lehmann et al. 2008), the monitored soil depth enables us to appropriately investigate the soil water dynamics in both the first and second stage.

Values of actual daily, E_a , and cumulative, $E_{a,c}$, evaporation are compared in Fig. 3 with the respective values of pan evaporation, E_{pan} , and $E_{pan,c}$, for two representative dry periods (4–12 May 2014 and 6–12 June 2014). These periods represent a typical evolution of the drying process in a natural bare plot starting from a condition of “well wet soil”. In fact, they are characterized by high initial soil water contents averaged along 35 cm soil depth, equal to 0.33 in May 4, 2014 and 0.32 in June 6, 2014, which are close to the saturation value, observed at 35 cm. Figure 3 displays the first stage of evaporation with coherent behavior of E_a and E_{pan}

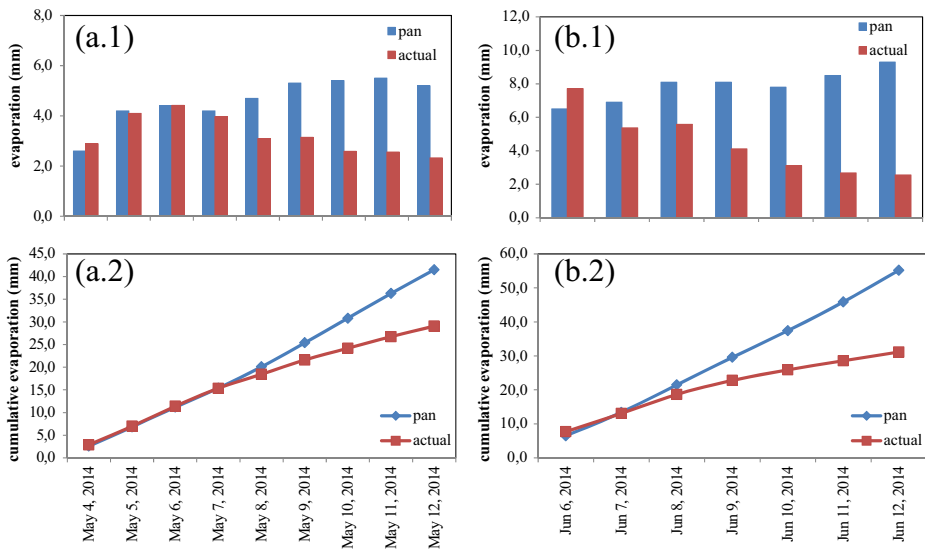


Fig. 3 Comparison of (1) the observed daily pan evaporation with the actual evaporation and (2) the corresponding cumulative quantities, during two drying periods: (a) May 4–12, 2014 and (b) June 6–12, 2014

values (clearer in Fig. 3a) and a second stage characterized by different trends. The second stage onset is clearly identified by a significant slope reduction exhibited by $E_{a,c}$. For the same dry periods the behavior of the ratio E_a/E_{pan} is also shown in Fig. 4, where it can be observed:

- a first stage of duration 3–4 days with E_a/E_{pan} characterized by a slight decrease in May which becomes more significant in June;
- a second stage with a gradual reduction of the evaporative flux towards an asymptotic threshold.

The behavior of E_a/E_{pan} observed in Fig. 4 matches the laboratory results obtained in columns filled with different porous media (Lehmann et al. 2008; Or et al. 2013; Assouline et al. 2014). Specifically, measured drying rates in an initially saturated soil exhibit first a climate-controlled stage with approximately constant or decreasing E_a equal to E_p and a posterior, second stage characterized by a significant evaporation reduction caused by the limiting soil water transport. The end of the first stage, and the onset of the second one, is clearly identified in Fig. 5 through the method suggested by Brutsaert and Chen (1995). In this figure the inverse of $(E_a/E_{pan})^2$ is represented as a function of time and the intercept between the line of linear regression and the ideal line joining those data points indicates the beginning of the second stage. The different behavior of E_a/E_{pan} observed in the first stage of the two dry periods, nearly time-invariant in May and decreasing in June, can be due to the higher atmospheric evaporative demand in the last period (see also Lehmann et al. 2008).

A further drying process observed in September 2014 reinforces our results. In this case (Fig. 6), the initial soil moisture averaged over 35 cm soil depth is lightly smaller (0.31) than in the previous two cases. The quantity E_a/E_{pan} exhibits again a decreasing trend with a transition stage (occurring after three days) but its evolution in time is fairly irregular.

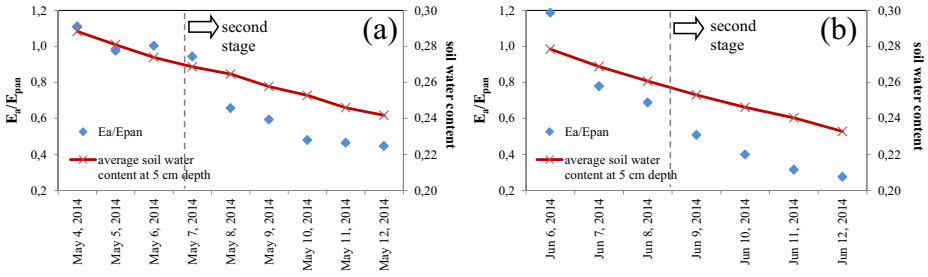


Fig. 4 Temporal evolution of actual daily evaporation, normalized through the pan evaporation, and average soil water content observed at 5 cm depth, during two drying periods: (a) May 4–12, 2014 and (b) June 6–12, 2014

4.2 Evidences on the Transition from the First to the Second Evaporation Stage

The time evolution of the normalized daily evaporation, E_a/E_{pan} , is plotted in Figs. 4 and 6b together with that of the average soil water content at the depth of 5 cm to highlight the coherent behavior between the two quantities. The depth of 5 cm has been selected following Wythers et al. (1999) who showed, for example, that at 14 days from the beginning of the dry period the evaporation from a bare soil had the greater influence on the upper 7.8 cm of a silt loam. From the analysis of Figs. 4 and 6b, we remark that:

- the average soil water content observed at 5 cm depth, starting from initial values of 0.29, 0.28 and 0.27 for the three dry periods, decreases slightly with a mean daily reduction tax of 5.8, 7.6 and 4.6 %, respectively, being affected to some degree by the external demand of evaporation rate;
- independently of the initial soil moisture, the transition from the first to the second evaporation stage occurs when the soil water content at 5 cm depth assumes values in a narrow range around 0.26, which could represent a critical threshold.

In order to support these deductions, two additional 10 days dry periods, occurred in June 2013 and October 2014, are considered in Fig. 7. These two periods are characterized by an initial soil water content averaged on 35 cm soil depth equal to 0.30 and 0.29, respectively, and soil moisture values at 5 cm very close to the above-

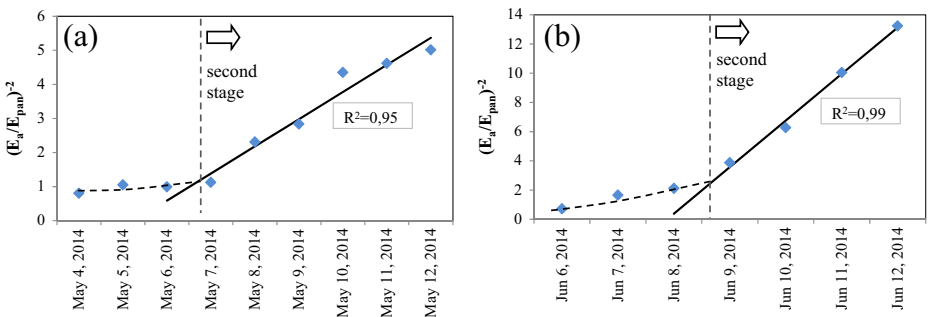


Fig. 5 Representation of the Brutsaert and Chen (1995) method to identify the onset of the second stage of the drying process (see text) for the two periods of Figs. 2 and 3. E_a/E_{pan} denotes the actual daily evaporation normalized through the pan evaporation. The continuous straight line represents the linear regression equation. The dotted line joins the earlier data points

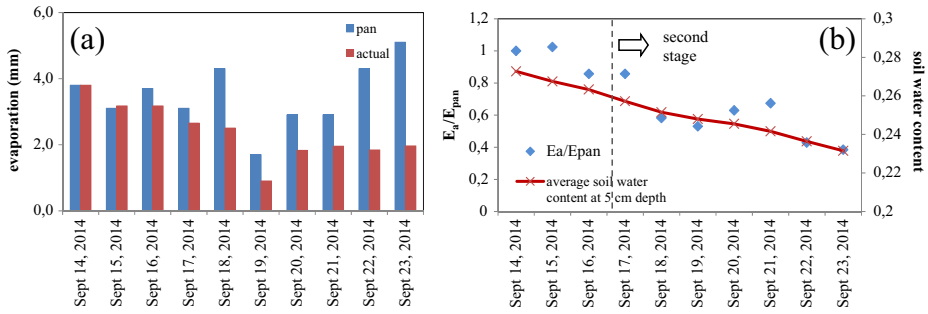


Fig. 6 (a) Comparison of the observed daily pan evaporation with the actual evaporation and (b) evolution in time of the actual evaporation normalized through the pan evaporation, for the drying period of September 14–23, 2014. The average soil water content observed at 5 cm depth is also given in (b)

mentioned critical threshold. As it can be appreciated in Fig. 7 the first stage of the evaporation process has not been detected. Since the beginning of the dry periods, the actual daily evaporation E_a is significantly lower than the pan value E_{pan} while the respective cumulative values $E_{a,c}$ and $E_{pan,c}$ diverge. Furthermore, the ratio E_a/E_{pan} remains almost invariable at very low values (around 0.23). On these bases, the hypothesis to express the break point between the first and the second stage of the evaporation process through a critical value of soil water content at a well-defined soil depth seems to be reasonable.

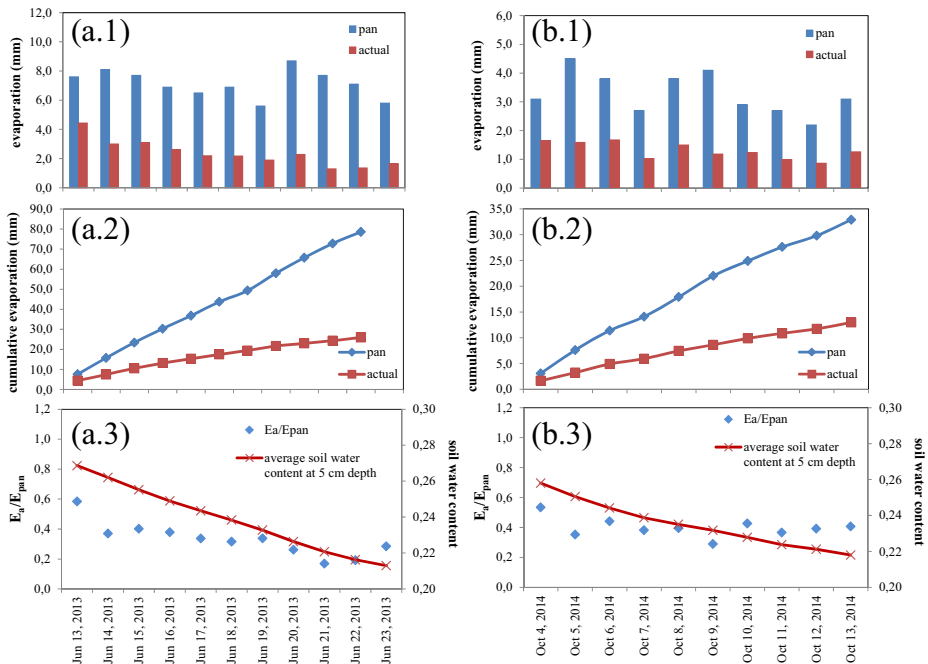


Fig. 7 Comparison of (1) the observed daily actual and pan evaporation depths and (2) of the corresponding cumulative values, for the dry periods of (a) June 13–23, 2013 and (b) October 4–13, 2014. (3) The temporal evolution of the actual daily evaporation, normalized through the pan evaporation, and that of the average soil water content observed at 5 cm depth are also shown

4.3 Determination of the Onset of the Second Evaporation Stage

In our experiments the first evaporation stage appears whenever the last rainfall event leaves a soil water content at 5 cm depth greater than a critical value (about 0.26 in our soil). The duration of this stage is typically in the range 3–4 days. The second evaporation stage starts next, when the soil water content at 5 cm depth drops below that critical threshold. Therefore, the average moisture at 5 cm depth in the study silt loam soil can be considered as an indicator of the transition between the first and second evaporation stage. We formulate the hypothesis that the critical value can be estimated through the soil field capacity (the soil water content at the capillary pressure of -0.33 bar), which represents the lower threshold for the soil drainage capability and has a role in the liquid hydraulic continuity conservation. Along this line, we described the soil retention curve through the following functional form (Morbidelli et al. 2012):

$$\psi(\theta) = \psi_b \left[\left(\frac{\theta - \theta_r}{\theta_s - \theta_r} \right)^{-\lambda} - 1 \right]^{\frac{1}{c}} + d \quad (2)$$

where θ_r and θ_s are the residual and saturated soil water contents, respectively, K_s is the saturated hydraulic conductivity, Ψ_b is the air entry head, λ is the Brooks–Corey pore size distribution index, c and d are empirical coefficients. Then, adopting for the involved hydraulic parameters the values of Table 1, we found a field capacity equal to 0.27, which is very close to the critical value deduced from the experiments.

As a further support to the above procedure based on the use of soil water content at 5 cm depth, for the dry period of May 2014 (Fig. 3a), we analyze in Fig. 8a the time evolution of the average soil water content at 5, 15, 25 and 35 cm soil depths and of the daily deep flow observed at 70 cm depth. The results can be summarized in three main points:

- the soil water content at 35 cm depth, which starts from the saturation value, is initially reduced due to the downward water movement caused by the gravitational component of the soil water potential. When the drainage rate vanishes, the less pronounced decreasing trend is due to the water supply upward;
- the soil water contents at 25 cm and 15 cm depths, to a lesser extent, show a behavior similar to that at the deepest level, 35 cm. Moisture values at the end of the dry period seem to asymptotically converge;
- the moisture content at 5 cm depth in a first stage exhibits almost a parallel decreasing tendency with respect to those of the greater depths, but with lower values, while after May 8, 2014, when the second stage starts (Fig. 4a), it experiences a more pronounced decrease.

In order to better clarify these aspects, Fig. 8b exhibits the daily relative decrease, RD, of soil moisture at different depths, z , with respect to the previous day, expressed as:

$$RD_{z,j} = \frac{\bar{\theta}_{z,j} - \bar{\theta}_{z,j-1}}{\bar{\theta}_{z,j-1}} \quad (3)$$

where $j > 1$ indicates the j -th day after the rainfall stops. At the end of the drainage process, relative decreases of the deeper levels, from 15 to 35 cm, tend to a limit, while the

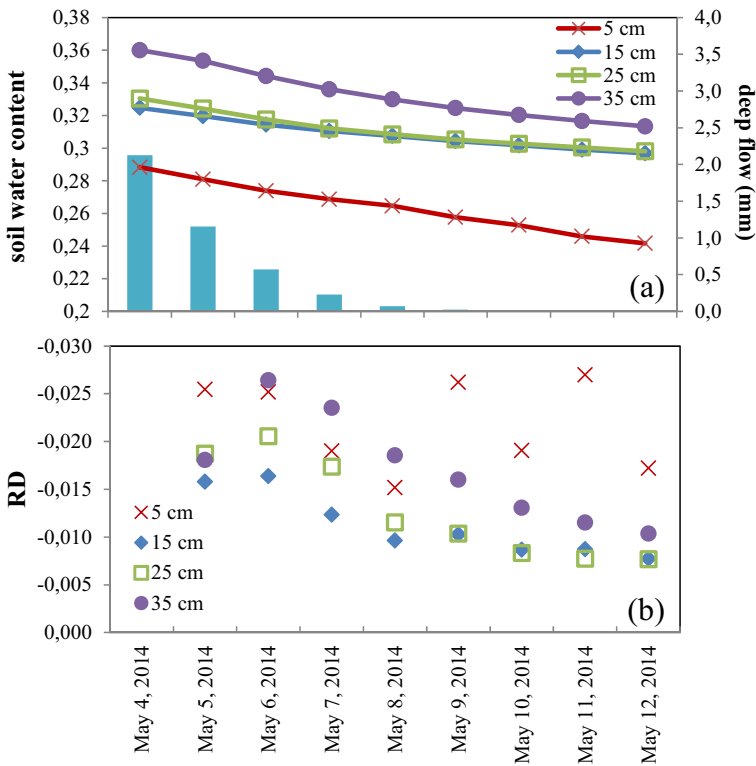


Fig. 8 Time evolution of (a) the average soil water content at different soil depths together with the deep flow observed at 70 cm depth and (b) the daily relative decrease, RD, in soil water content with respect to the previous day at different depths *z*, during the dry period of May 4–12, 2014 (see also Figs. 2a–3a)

near surface values exhibit an irregular behavior possibly due to fluctuations of atmospheric conditions. The different behavior becomes significant after May 8, 2014 when the soil water content at 5 cm depth approaches the field capacity value as a result of a decrease of the liquid hydraulic continuity in the upper soil layer. The overall analysis of Fig. 8 confirms that in the study silt loam soil the measurement of water content at 5 cm depth is a good indicator of the progress of the evaporation process, at least in the first two stages.

We note that the results above synthesized allow us to describe the evaporation process for dry period lengths shorter than the maximum considered value (11 days) that involve only the first stage or both the first and the second stage, while for greater lengths the third stage with very low evaporation rates has to be represented.

4.4 Relationship among Pan Evaporation, Potential Evaporation and Actual Evaporation

An overview of the results presented in Figs. 3 and 6 suggests that pan evaporation can be an effective estimator of actual evaporation, at least during the first stage of the process, when the potential evaporation rate occurs. This fact is supported by the coherent trends of actual and pan evaporation in May 4–8, 2014, June 6–8, 2014 and

September 14–17, 2014. The normalized actual daily evaporation, E_a/E_{pan} , is plotted against the average soil water content at 5 cm depth in Fig. 9 for all the dry days of the observation period (May–September 2010, June–July 2013 and May–October 2014). By using the threshold of field capacity (0.27) for the end of the first stage of soil water evaporation, we selected (Fig. 9) the dry days with average soil water content at 5 cm depth greater than 0.27 and therefore characterized by evaporation rate approaching the potential value. Then, by averaging the corresponding E_a/E_{pan} values we derived a proportionality coefficient between pan and potential evaporation equal to 1.04. This result substantially agrees with that obtained through in mixed natural vegetated soils (Kahler and Brutsaert 2006). On the other hand, Fig. 9 shows how E_a/E_{pan} has a well-defined non-linear trend for values of soil moisture smaller than the field capacity. This indicates that accurate pan evaporation measurements combined with appropriate soil moisture observations can provide helpful insights on the representation of evaporation process from natural bare soils through the different stages.

5 Conclusions

Actual daily evaporation rates, E_a , derived by the application of the hydrological balance equation in a plot with a bare silt loam soil have been scaled with pan evaporation measurements, E_{pan} , that have been considered representative of the atmospheric evaporative demand. The evolution in time of E_a/E_{pan} in dry summer periods has been analyzed as a function of the soil moisture profile. The results suggest that the soil moisture observed at an appropriate depth, 5 cm for a silt loam soil, can be considered an effective indicator of the first two evaporation stages. In this context the field capacity plays a fundamental role. The initial soil moisture affects the conservation or loss of the liquid hydraulic continuity at different depths during the drying process.

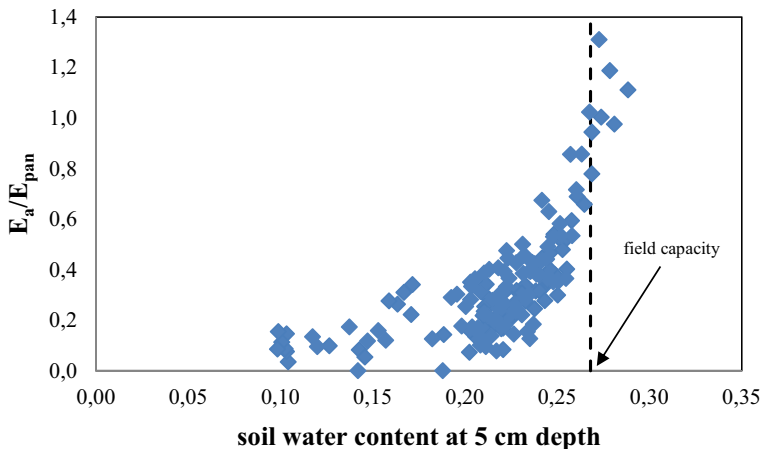


Fig. 9 Actual daily evaporation, normalized with pan measurements, as a function of the average soil water content at 5 cm depth for the dry days of the observation period (May–September 2010, June–July 2013 and May–October 2014)

Accurate pan evaporation measurements give good estimates of E_a in the first stage of the process and exhibit, through the soil water content observed at a proper depth, a clear correlation with E_a even in the successive phases.

Our results provide insights on the crucial quantities to be measured in field to pursue a reliable representation of the evaporation process in bare silt loam soils.

This study limited to silt loams should be extended to a variety of natural bare soils.

Acknowledgments This research was mainly financed by the Italian Ministry of Education, University and Research (PRIN 2015: Innovative monitoring and design strategies for sustainable landslide risk mitigation).

References

- Allen RG, Pereira LS, Raes D, Smith M (1998) Crop evapotranspiration. Guidelines for computing crop water requirements. FAO Irrigation and Drainage Paper No. 56, Rome
- Aminzadeh M, Roderick ML, Or D (2016) A generalized complementary relationship between actual and potential evaporation defined by a reference surface temperature. *Water Resour Res* 52(1):385–406. <https://doi.org/10.1002/2015WR017969>
- Assouline S, Narkis K, Gherabli R, Lefort P, Prat M (2014) Analysis of the impact of surface layer properties on evaporation from porous systems using column experiments and modified definition of characteristic length. *Water Resour Res* 50(5):3933–3955. <https://doi.org/10.1002/2013WR014489>
- Balugani E, Lubczynski MW, Metselaar K (2016) A framework for sourcing of evaporation between saturated and unsaturated zone in bare soil condition. *Hydrol Sci J* 61(11):1981–1995. <https://doi.org/10.1080/02626667.2014.966718>
- Banimahd SA, Khalili D, Kamgar-Haghighi AA, Zand-Parsa S (2016) Evaluation of groundwater potential recharge models considering estimated bare soil evaporation, in a semi-arid foothill region. *Hydrol Sci J* 61(1–2):162–172. <https://doi.org/10.1080/02626667.2014.959957>
- Berretta C, Poë S, Stovin V (2014) Moisture content behavior in extensive green roofs during dry periods: the influence of vegetation and substrate characteristics. *J Hydrol* 516:37–49. <https://doi.org/10.1016/j.jhydrol.2014.04.001>
- Bittelli M, Ventura F, Campbell GS, Snyder RL, Gallegati F, Pisa PR (2008) Coupling of heat, water vapor, and liquid water fluxes to compute evaporation in bare soils. *J Hydrol* 362(3–4):191–205. <https://doi.org/10.1016/j.jhydrol.2008.08.014>
- Brutsaert W, Chen D (1995) Desorption and the two stages of drying of natural tallgrass prairie. *Water Resour Res* 31(5):1305–1313. <https://doi.org/10.1029/95WR00323>
- Griffoll J, JMa G, Cohen Y (2005) Non-isothermal soil water transport and evaporation. *Adv Water Resour* 28(11):1254–1266. <https://doi.org/10.1016/j.advwatres.2005.04.008>
- Idso SB, Reginato RJ, Jackson RD, Kimball BA, Nakayama FS (1974) The three stages of drying of a field soil. *Soil Sci Soc Am Proc* 38(5):831–837. <https://doi.org/10.2136/sssaj1974.03615995003800050037x>
- Jalota SK, Prihar SS (1986) Effects of atmospheric evaporativity, soil type and redistribution time on evaporation from bare soil. *Aust J Soil Res* 24(3):357–366. <https://doi.org/10.1071/SR9860357>
- Kahler DM, Brutsaert W (2006) Complementary relationship between daily evaporation in the environment and pan evaporation. *Water Resources Research* W05413 42(5):1–9
- Lehmann P, Assouline S, Or D (2008) Characteristic lengths affecting evaporative drying of porous media. *Phys Rev E Stat Nonlinear Soft Matter Phys* 77(5):1–15
- Lemon ER (1956) The potentialities for decreasing soil moisture evaporation loss. *Soil Sci Soc Am Proc* 20(1): 120–125. <https://doi.org/10.2136/sssaj1956.03615995002000010031x>
- Linsley RK, Franzini JB, Freyberg DL, Tchobanoglous G (1992) *Water resources engineering*. McGraw-Hill, Singapore
- McVicar TR, Roderick ML, Donohue RJ, Li LT, Van Niel TG, Thomas A, Grieser J, Jhajharia D, Himri Y, Mahowald NM, Mescherskaya AV, Kruger AC, Rehman S, Dinpashoh Y (2012) Global review and synthesis of trends in observed terrestrial near-surface wind speeds: implications for evaporation. *J Hydrol* 416–417:182–205. <https://doi.org/10.1016/j.jhydrol.2011.10.024>
- Melone F, Corradini C, Morbidelli R, Saltalippi C (2006) Laboratory experimental check of a conceptual model for infiltration under complex rainfall patterns. *Hydrol Process* 20(3):439–452. <https://doi.org/10.1002/hyp.5913>

- Morbidelli R, Corradini C, Saltalippi C, Flammini A, Rossi E (2011) Infiltration-soil moisture redistribution under natural conditions: experimental evidence as a guideline for realizing simulation models. *Hydrol Earth Syst Sci* 15(9):2937–2945. <https://doi.org/10.5194/hess-15-2937-2011>
- Morbidelli R, Corradini C, Saltalippi C, Brocca L (2012) Initial soil water content as input to field-scale infiltration and surface runoff models. *Water Resour Manag* 26(7):1793–1807. <https://doi.org/10.1007/s11269-012-9986-3>
- Novak MD (2010) Dynamics of the near-surface evaporation zone and corresponding effects on the surface energy balance of a drying bare soil. *Agric For Meteorol* 150(10):1358–1365. <https://doi.org/10.1016/j.agrformet.2010.06.005>
- Or D, Lehmann P, Shahraeeni E, Shokri N (2013) Advances in soil evaporation physics—a review. *Vadose Zone J* 12(4):1–16
- Philip JR, de Vries DA (1957) Moisture movement in porous materials under temperature gradients. *Transactions American Geophysical Union* 38(2):222–232. <https://doi.org/10.1029/TR038i002p00222>
- Rotsatyn LD, Roderick ML, Farquhar D (2006) A simple pan-evaporation model for analysis of climate simulations: evaluation over Australia. *Geophys Res Lett* 33(17):L17715. <https://doi.org/10.1029/2006GL027114>
- Shokri N, Lehmann P, Or D (2010) Evaporation from layered porous media. *Journal of Geophysical Research: Solid Earth* 115(6):B06204
- Shokri N, Sahimi M, Or D (2012) Morphology, propagation dynamics and scaling characteristics of drying fronts in porous media. *Geophysical Research Letters* L09401 39(9):1–5
- Wythers KR, Lauenroth WK, Paruelo JM (1999) Bare-soil evaporation under semiarid field conditions. *Soil Sci Soc Am J* 63(5):1341–1349. <https://doi.org/10.2136/sssaj1999.6351341x>